PROCEEDINGS OF SCIENCE

Isotopic Production Cross Section Updates in GALPROP for Supporting TIGERISS

P. Ghosh[d,e,h,*], I. V. Moskalenko[k], T. Porter[k], J. F. Krizmanic[d], R. F. Borda[a], R. G. Bose[b], D. L. Braun[b], J. H. Buckley[b], J. Calderon[c], N. W. Cannady[a,d,e], R. M. Caputo[d], S. Coutu[f], G. A. de Nolfo[g], S. Jones[c], C. A. Kierans[d], W. Labrador[b], L. Lisalda[b], J. V. Martins[a], M. P. McPherson[i], E. Meyer[a], J. W. Mitchell[d], S. I. Mognet[f], A. Moiseev[j,d,e], S. Nutter[c], I. Pastrana[b], B. F. Rauch[b], H. Salmani[i], M. Sasaki[j,d,e], G. E. Simburger[b], S. Smith[h], H. A. Tolentino[i], D. Washington[f], W. V. Zober[b]

[a] *University of Maryland, Baltimore County, MD 21250, USA*
[b] *Washington University in St. Louis, MO 63130 USA*
[c] *Northern Kentucky University, Highland Heights, KY 41099 USA*
[d] *NASA Goddard Space Flight Center, Astrophysics Science Division, Greenbelt, MD 20771 USA*
[e] *Center for Research and Exploration in Space Sciences and Technology II, Greenbelt, MD 20771 USA*
[f] *Pennsylvania State University, University Park, PA 16801, USA*
[g] *NASA Goddard Space Flight Center, Heliophysics Science Division, Greenbelt, MD 20771 USA*
[h] *Catholic University of America, Washington DC 20064, USA*
[i] *Howard University, Washington DC 20059, USA*
[j] *University of Maryland, College Park, MD 20742, USA*
[k] *Stanford University, Stanford, CA 94305 USA*
E-mail: priyarshini.ghosh@nasa.gov

The PIONEERS-selected mission TIGERISS, planned to launch to the ISS in 2026, will provide, for the first time, single-element resolution Galactic cosmic-ray elemental abundances spanning the periodic table, from $_{5}$B up to $_{82}$Pb, to further our understanding of the grand cycle of matter in the Galaxy. Such wide-range, fine-resolution experimental data would be best combined with the latest developments in astrophysical models, but the current accuracy of nuclear isotopic production cross sections is far behind the accuracy delivered by space instrumentation. We are updating the current cross section library employed by the GALPROP framework for propagation of Galactic cosmic rays and diffuse emissions with newer reaction channels and more accurate data on existing channels that have been reported over the last two decades. This will provide a crucial update to the state-of-the-art tool widely used by the community to explore the information encoded in the chemical composition of cosmic rays. Our main focus are the proton spallation reactions on 1) isotopes of $_{5}$B through $_{82}$Pb, and 2) the sub-Fe group; we are also concentrating on

38th International Cosmic Ray Conference (ICRC2023)
26 July - 3 August, 2023
Nagoya, Japan

*Speaker

PoS(ICRC2023)049

the electron-capture isotopes which provide additional constrains on the processes involving energy gain and loss by cosmic rays species in the interstellar medium and the heliosphere.

1. Introduction

Galactic Cosmic Rays (GCRs) carry information about how the Galaxy produces and distributes different elements, and they are one of the few direct samples of matter from outside the solar system. Excellent elemental abundance data up to Z = 30 are presently available from various instruments, such as ACE-CRIS [1], AMS-02 [2-7], CALET [8-10], etc. For 30<Z<60, results from TIGER [11] and SuperTIGER [12] must be combined with measured data from missions such as HEAO-HNE and ACE-CRIS to clearly show the continuous separation of refractory and volatile elements. The relative rarity of GCRs at higher charges makes individual elemental abundances of Ultra-Heavy GCR (UHGCR) above nuclear charge Z = 56 difficult to measure and remain unknown. The only are available for Z > 60 with single element resolution at the highest charges were obtained by the Trek [13] detector on MIR space station, which however are almost impossible to normalize, given the lack of other comparable measurements and Trek's sensitivity to Z > ~70.

The Trans-Iron GalacticElement Recorder for the International Space Station (TIGERISS) will address the scarcity of UHGCR data in several ways [14]. Firstly, by combining Silicon Strip Detectors and Cherenkov detectors, TIGERISS will be ableto measure charge with uncertainty on the order of 0.2 charge units from $_{5}$B up to $_{82}$Pb (Fig. 1). This unprecedented fine resolution for the UHGCR range will allow TIGERISS to separate abundant even-charged nuclei from rarer odd-charged nuclei. Additionally, the wide range of measurementsfrom a single instrument enables normalization that resolves discrepancies between previous instruments, such as that of ACE-CRIS and SuperTIGER/CALET. Lastly, TIGERISS will have lesser systematic uncertainties, primarily due to the absenceof atmospheric overburden on the ISS.

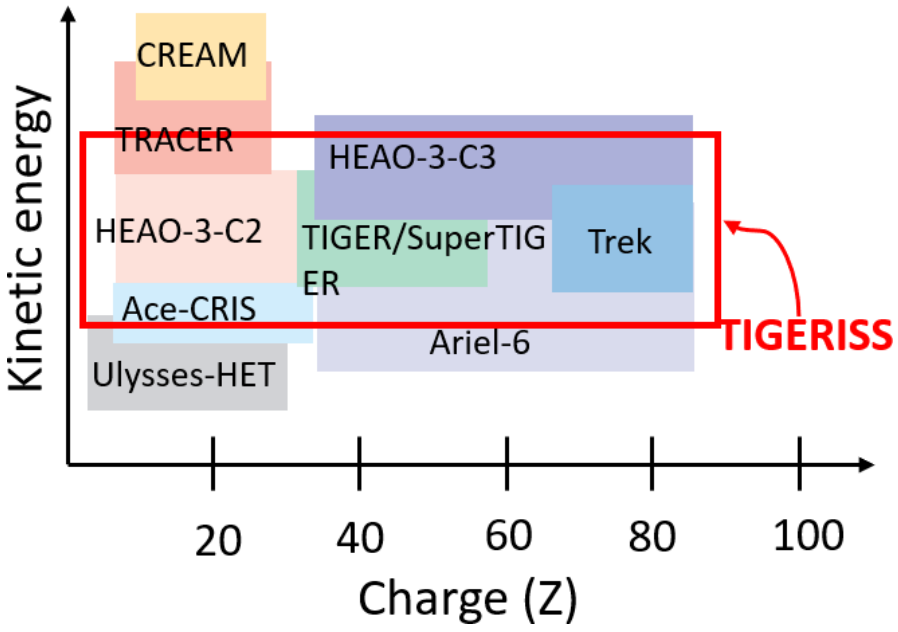

Figure 1: TIGERISS will be the first instrument to measure UHGCR abundances from B to Pb with single-element resolution, thus eliminating the need for normalization with other measurements.

Equipped with such first-of-its-kind capabilities, TIGERISS aims to provide insight into astrophysical nucleosynthesis; specifically, to address questions about the origins of r-process nuclei

and the contributions of these origins to the Galactic r-process budget, and the limits of CR nucleosynthesis and acceleration in OB associations. Our understanding of the Galactic composition and GCR propagation has come a long way since the advent of analytical and semi- analytical techniques, and with the continuous flow of new and more accurate data from space, balloon and ground-based measurements, there is a need for models that incorporate the complexities of propagation of GCRs. To model such complex phenomena, the numerical code GALPROP [15,16] calculates the propagation of relativistic charged particles and the diffuse emissions produced during their propagation. The code incorporates vast information from astrophysics, nuclear and particle physics with the main goal to be as realistic as possible and combines it with the latest theoretical developments. GALPROP works by calculating the propagation of cosmic-ray nuclei, antiprotons, electrons and positrons, and computes diffuse γ- rays and synchrotron emission in the same framework. While the experimental data from TIGERISS will enable GALPROP to better constrain cosmic ray propagation, the key element is the accuracy of the cross-section (CS) data available, which becomes a bottleneck in the identification and interpretation of subtle features associated with Galactic cosmic rays, thereby necessitating careful and continuous updating of CS data.

1.1 Updating Cross Sections in GALPROP

The routines for the isotopic production cross sections are built using a systematic approach tuned to all available data extracted from Los Alamos (LANL) and Experimental Nuclear Reaction Data (EXFOR) databases, as well as from an extensive literature search (1950-2002). To account for different measurement techniques that were introduced in experimental nuclear physics over decades of research since the 1950s, the distinction was made between the individual, direct, decaying, charge-changing, cumulative, differential, total, and isobaric cross sections, or reactions with metastable final states, with the target that could be a particular isotope, a natural sample with mixed isotopic composition, or a chemical compound. Often, experimental cross sections for the same reaction published by various groups were found to differ by a significant factor. A (tough) decision on which set to be used was based on examination of the descriptions of particular experimental setups in the original papers. For details and references see [21].

The most effort was devoted to the main contributing channels. The approach to the description of each channel depended on the accuracy and availability of experimental data. If the cross-section data were detailed enough, they were approximated with fitted functional dependences or provided as a table for interpolation. If only a few or no data points were available, such cross sections were approximated using the results of the Los Alamos nuclear codes, such as a version of the Cascade-Exciton Model (CEM2k) and the ALICE code with the Hybrid Monte Carlo Simulation model (HMS-ALICE). Parameterizations of all isotopic production cross sections are provided from a few MeV/nucleon to several GeV/nucleon, above which they are assumed to be constant.

In the case of a minor contribution channel, the best of the available semiempirical formulae by Webber et al. (WNEWTR [22]) or parametric formulae by Silberberg and Tsao (YIELDX code[23]) normalized to the data when they exist was used. Each of the thousands of channels was tested to ensure the best description of the available data. A very limited database of the measured cross-section points (~2,000) is supplied with GALPROP routines to renormalize the output of WNEWTR and YIELDX codes. The data points to include in this database were selected for the stated validity range of the semiempirical formulae (typically >150

MeV/nucleon), while the data points outside of this validity range were excluded from the auxiliary files.

Over the last 20 years, many new experiments have been performed, with newly measured reaction channels, and more accurate cross-section data on existing channels. Given TIGERISS' capability of measuring elemental abundance up to $_{82}$Pb, there is an ongoing effort to add high Z spallation reactions above Z = 30. Furthermore, based on the continued inconsistencies in the calculated rates of reacceleration in the interstellar medium between observations of the ^{51}V/^{51}Cr and ^{49}Ti/^{49}V ratios, [17] and [18] have repeatedly hypothesized that the inconsistencies are a result of large uncertainties in existing fragmentation cross sections. In fact, [19, 20] postulated that reducing the ^{49}Ti fragmentation cross-section by 15% would resolve the discrepancy. Therefore, the other area of interest is the electron-capture isotopes in the sub-Fe group that can be used to study energy-dependent propagation, such as diffusive reacceleration in the interstellar medium (ISM) and heliospheric modulation.

1.1.1 Methodology of Data Selection

Numerous experiments report CS data for reactions; some add to previously existing data and reaction channels, some report completely new reactions. Comprehensive lists of CS data are extracted from libraries such as Evaluated Nuclear Data File (ENDF) [24], Experimental Nuclear Reaction Data (EXFOR) [25], the Landolt-Börnstein series [26], from experiments performed all over the world, such as at GSI in Darmstadt, Germany, the Bevatron at Lawrence Berkeley Laboratory in California, USA, the Clinton P. Anderson Meson Physics Facility at Los Alamos National Laboratory in New Mexico, USA, amongst many others. It would be an overwhelming task to gather data from the large number of sources online, therefore it is imperative to have a systematic sorting of data, so the appropriate measurements can be selected. Several parameters determine the limitations of the CS data and their relevancy for our purposes. Below, are certain parameters that help us decide which data to select and which to discard:

1. Cross section type: individual (the probability of a nuclear interaction resulting in a daughter nuclide only), cumulative (a sum of cross sections of all reaction channels on a well-defined target nucleus which leads to direct production of the final nuclide), decayed (the same final nuclide can also be produced indirectly via the decay of progenitors produced simultaneously on the target nucleus), metastable states (decayed daughter isotopes in isomeric states versus in ground states), charge-changing (when the reaction results in a change of charge Z), mass-changing (when the reaction results in a change of mass A). Data with different types of cross sections cannot be lumped together.
2. Type of experiment performed: direct and reverse kinematics. In direct kinematic experiments, heavy projectiles are accelerated to cosmic-ray velocities, representing the primary cosmic ray nucleus, and are bombarded on a stationary hydrogen target representing the ISM, such as a liquid H_2 target. While this type of interaction is an exact representation of cosmic-ray interaction in the ISM, the safety and maintenance costs of liquid H are prohibitively high, or target subtractions are necessary if CH_4 targets are used instead. The solution to this dilemma is to use reverse kinematics, where the assumption is made that the ISM is mostly hydrogen, and hence a 'moving' ISM (proton beam) is accelerated towards a fixed cosmic ray (nuclear target). Although this setup is much simpler and cost-effective, the method assumes no collective effect in the target including molecular effects,

and it is the reverse of how CR interactions take place in the ISM. The type of experiment performed can have a strong bearing on the errors reported, thereby dictating the relevancy of the experimental data to be included.

3. Uncertainty: errors can be of the systematic kind (determined by factors such as beam purity, intensity fluctuations, target purity, spectrometer calibration, detector efficiency, self-absorption of γ-rays in sample, interference from secondary particles) or statistical (determined by lower cross sections, detector count rates, correction of unresolved γ-ray lines, background under spectral peak, spectrometer dead time and count loss, total error of the nuclide production rate, etc.)

We also emphasize the use of low-energy data. Previously, the CS data at <100 MeV/nucleon was often ignored because all available CR data was taken inside the heliosphere and the modulation potential is ~400 MV at the solar minimum thus setting the lowest ISM energy of detected particles at ~200 MeV/nucleon. However, they have garnered interest since Voyager 1, 2 entered the ISM and data down to a few MeV/nucleon becomes available. Secondly, propagation models currently in use include energy changing processes such as stochastic re-acceleration (gain) and ionization losses, and, therefore, low-energy cross section behavior becomes important.

Once the appropriate CS data has been selected, they are then parametrized into continuous cross-section data across the energy range of interest using several schemes such as re-normalized fits of Silverberg and Tsao's code or Webber's code (according to their energy range of validity), empirical fits based on available data, and on theoretical calculations.

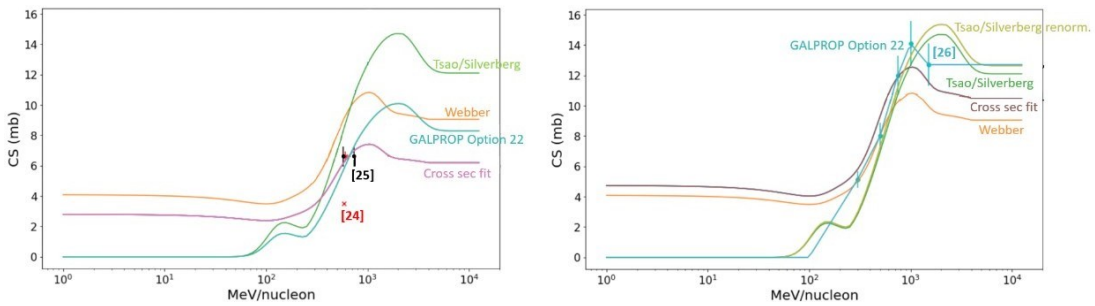

Figure 2. Parameterization for $^{56}Fe + p$ --> ^{40}K in GALPROP using (left) older data, and (right) newer, more accurate data.

Fig. 2 shows the cross section parametrization for the reaction $^{56}\mathrm{Fe} + p$ --> $^{40}\mathrm{K}$. The left panel shows parametrization fits and schemes for older data of cumulative cross sections from [27] (in red) which reported no uncertainty, and from [28] (in black) whose beam purity was not reported with well-defined systematic uncertainty. Webber and Silverberg/Tsao's parameterizations don't agree well with the four data points; in this minor channel and just four data points, GALPROP also employs one of those renormalized approximations. The right panel shows the parametrization using newer individual cross section data from [29] (in purple). The cross section renormalization misses the highest two data points from [29], Tsao/Silverberg's fit matches closer with the data than Webber's. It also shows the updated approximation passing through all data points.

Finally, Fig. 3 shows the current status of reaction channels in GALPROP's CS library. Green pixels represent reaction channels that are already present in v57 version of GALPROP

that is available online. Red pixels represent reaction channels that are present in the v57 version and used for renormalization of the Webber and Silverberg/Tsao's parameterizations, but newer, more accurate data has been made available for the existing channel and are being incorporated into the library. Yellow pixels represent new measured reaction channels. Efforts are ongoing to add more reaction channels to the sub-Fe group and Z >30.

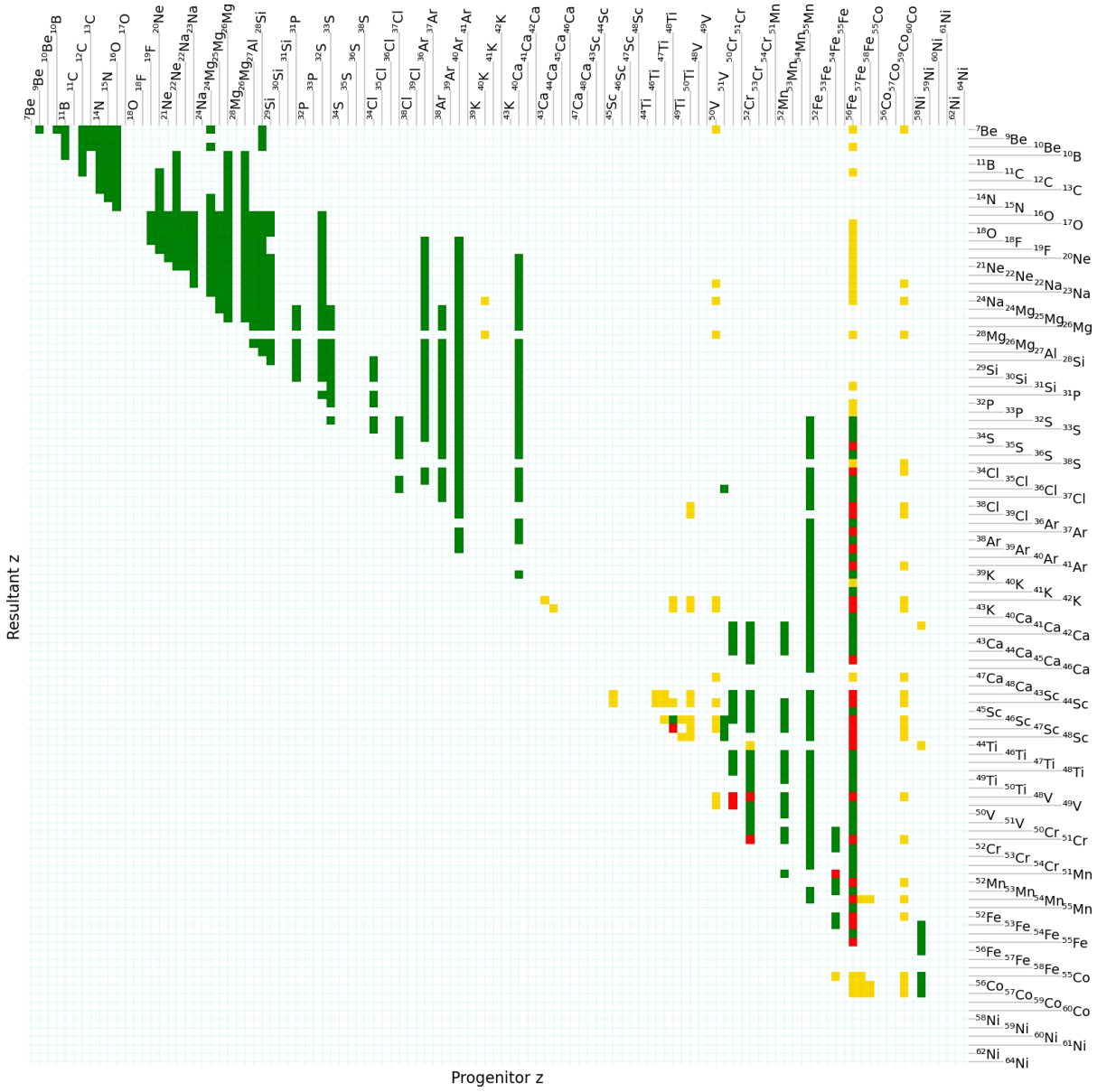

Figure 3. Reaction channels for proton spallation of isotopes up to Z = 30.

Acknowledgement

This work was supported by NASA under grants NNX09AC17G, NNX09AC18G, NNX14AB24G, NNX14AB25G, and NNX15AC15G. IVM and TAP acknowledge partial support from NASA grants Nos. 80NSSC22K0477, 80NSSC22K0718, 80NSSC23K0169.

References

[1] K. A. Lave et al., " GALACTIC COSMIC RAY ENERGY SPECTRA AND COMPOSITION DURING THE 2009 2010 SOLAR MINIMUM PERIOD," ApJ, vol. 770, no . 2, p. 117, Jun. 2013, doi: 10.1088/0004 637X/770/2/117

[2] M. Aguilar et al., "ISOTOPIC COMPOSITION OF LIGHT NUCLEI IN COSMIC RAYS: RESULTS FROM AMS-01," ApJ, vol. 736, no. 2, p. 105, Aug. 2011, doi: 10.1088/0004-637X/736/2/105

[3] M. Aguilar et al., "Properties of Cosmic Helium Isotopes Measured by the Alpha Magnetic Spectrometer," Phys. Rev. Lett., vol. 123, no. 18, p. 181102, Nov. 2019, doi: 10.1103/PhysRevLett.123.181102

[4] M. Aguilar et al., "Properties of a New Group of Cosmic Nuclei: Results from the Alpha Magnetic Spectrometer on Sodium, Aluminum, and Nitrogen," Phys. Rev. Lett., vol. 127, no. 2, p. 021101, Jul. 2021, doi: 10.1103/PhysRevLett.127.021101

[5] M. Aguilar et al., "Precision Measurement of the Boron to Carbon Flux Ratio in Cosmic Rays from 1.9 GV to 2.6 TV with the Alpha Magnetic Spectrometer on the International Space Station," Phys. Rev. Lett., vol. 117, no. 23, p. 231102, Nov. 2016, doi: 10.1103/PhysRevLett.117.231102.

[6] M. Aguilar et al., "Properties of Heavy Secondary Fluorine Cosmic Rays: Results from the Alpha Magnetic Spectrometer," Phys. Rev. Lett., vol. 126, no. 8, p. 081102, Feb. 2021, doi: 10.1103/PhysRevLett.126.081102

[7] M. Aguilar et al., "Properties of Iron Primary Cosmic Rays: Results from the Alpha Magnetic Spectrometer," Phys. Rev. Lett., vol. 126, no. 4, p. 041104, Jan. 2021, doi: 10.1103/PhysRevLett.126.041104

[8] O. Adriani et al., "Direct Measurement of the Cosmic-Ray Proton Spectrum from 50 GeV to 10 TeV with the Calorimetric Electron Telescope on the International Space Station," Phys. Rev. Lett., vol. 122, no. 18, p. 181102, May 2019, doi: 10.1103/PhysRevLett.122.181102.

[9] O. Adriani et al., "Direct Measurement of the Cosmic-Ray Carbon and Oxygen Spectra from 10 GeV / n to 2.2 TeV / n with the Calorimetric Electron Telescope on the International Space Station," Phys. Rev. Lett., vol. 125, no. 25, p. 251102, Dec. 2020, doi: 10.1103/PhysRevLett.125.251102.

[10] O. Adriani et al., "Measurement of the Iron Spectrum in Cosmic Rays from 10 GeV / n to 2.0 TeV / n with the Calorimetric Electron Telescope on the International Space Station," Phys. Rev. Lett., vol. 126, no. 24, p. 241101, Jun. 2021, doi: 10.1103/PhysRevLett.126.241101.

[11] B. F. Rauch et al., "COSMIC RAY ORIGIN IN OB ASSOCIATIONS AND PREFERENTIAL ACCELERATION OF REFRACTORY ELEMENTS: EVIDENCE FROM ABUNDANCES OF ELEMENTS 26 Fe THROUGH 34 Se," ApJ, vol. 697, no. 2, pp. 2083–2088, Jun. 2009, doi: 10.1088/0004-637X/697/2/2083.

[12] R. P. Murphy et al., "GALACTIC COSMIC RAY ORIGINS AND OB ASSOCIATIONS: EVIDENCE FROM SuperTIGER OBSERVATIONS OF ELEMENTS 26 Fe THROUGH 40 Zr," ApJ, vol. 831, no. 2, p. 148, Nov. 2016, doi: 10.3847/0004-637X/831/2/148.

[13] A. J. Westphal, P. B. Price, B. A. Weaver, and V. G. Afanasiev, "Evidence against stellar chromospheric origin of Galactic cosmic rays," Nature, vol. 396, no. 6706, pp. 50–52, Nov. 1998, doi: 10.1038/23887.

[14] N. E. Walsh, "PhD. Thesis: SuperTIGER Elemental Abundances for the Charge Range $41 \leq Z \leq 56$." Washington University, 2020.

[15] A.W. Strong, I.V. Moskalenko, "Models for Galactic cosmic-ray propagation", Advances in Space Research, Volume 27, Issue 4, 2001, Pages 717-726, ISSN 0273-1177.

[16] Moskalenko, Igor & Jóhannesson, Gudlaugur & Orlando, Elena & Porter, Troy & Strong, A.W.. (2017). GALPROP Code for Galactic Cosmic Ray Propagation and Associated Photon Emissions. 279. 10.22323/1.301.0279.

[17] F. C. Jones, A. Lukasiak, V.S. Ptuskin, W.R. Webber, K-capture cosmic ray secondaries and reac-celeration, Advances in Space Research, Volume 27, Issue 4, 2001, Pages 737-741, ISSN 0273- 1177, https://doi.org/10.1016/S0273-1177(01)00113-2.

[18] Niebur S. M., Binns W. R., Christian E. R. et al. 2001 Proc. ICRC (Hamburg) 5 1675

[19] Niebur, S. M., et al. (2003), Cosmic ray energy loss in the heliosphere: Direct evidence from electron-capture-decay secondary isotopes, J. Geophys. Res., 108, 8033, doi:10.1029/2003JA009876, A10.

[20] Benyamin, D., Shaviv, N.J., and Piran, T. Electron-capture Isotopes Could Constrain Cosmic-Ray Propagation Models. The Astrophysical Journal, vol. 851, 2017, pp.109 -115.

[21] Boschini, M. J., et al. Inference of the Local Interstellar Spectra of Cosmic-Ray Nuclei Z≤28 with the GALPROP-HELMOD Framework. The Astrophysical Journal Supplement 250 (2020) 27.

[22] Webber, W. R., Soutoul, A., Kish, J. C., & Rockstroh, J. M. 2003, ApJS, 144, 153

[23] Tsao, C. H., Silberberg, R., & Barghouty, A. F. 1998, ApJ, 501, 920

[24] https://www-nds.iaea.org/exfor/endf.htm

[25] https://www-nds.iaea.org/exfor/

[26] Landolt-Börnstein_I-13d_Interactions of Protons with Nuclei (Supplement to I-13a,b,c)

[27] Chackett, K. F.: Yields of Potassium Isotopes in High Energy Bombardments of Vanadium, Iron, Cobalt, Nickel, Copper and Zinc, J. Inorg. Nucl. Chem. 27 (1965) 2493.

[28] Webber, W. R., Kish, J. C., Schrier, D. A., Total charge and mass changing cross sections of relativistic nuclei in hydrogen, helium and carbon targets. Physical Review C, vol. 41, no. 2, 1990.

[29] Villagrasa-Canton, C. & Boudard, A. & Ducret, J.E. & Fernandez, Belkis & Leray, Sylvie & Volant, C. & Armbruster, P. & Enqvist, Timo & Hammache, F. & Helariutta, K. & Jurado, B. & Ric-ciardi, M.-V & Schmidt, K.-H & Sümmerer, K. & Vivès, F. & Yordanov, O. & Audouin, Laurent & Bacri, C.-O & Ferrant, L. & Junghans, A.. (2007). Spallation residues in the reaction 56Fe+p at 0.3A,0.5A,0.75A,1.0A, and 1.5A GeV. Phys. Rev. C. ?? volume, pages.